LA-UR-87-1452

Los Alamos National Laboratory is operated by the University of California for the United States Department of Energy under contract W-7405-ENG-36

LA-UR--87-1452

DE87 009012

TITLE Photoconductor Pulse Generators and Sampling Gates for Characterization of High-Speed Devices and Transmission Lines

AUTHOR(S) N. G. Paulter and R. B. Hammond

SUBMITTED TO SPIE Proceedings

DISCLAIMER

This report was prepared as an account of work sponsored by an agency of the United States Government. Neither the United States Government nor any agency thereof, nor any of their employees, makes any warranty, express or implied, or assumes any legal liability or responsibility for the accuracy, completeness, or usefulness of any information, apparatus, product, or process disclosed, or represents that its use would not infringe privately owned rights. Reference herein to any specific commercial product, process, or service by trade name, trademark, manufacturer, or otherwise does not necessarily constitute or imply its endorsement, recommendation, or favoring by the United States Government or any agency thereof. The views and opinions of authors expressed herein do not necessarily state or reflect those of the United States Government or any agency thereof.

By acceptance of this article the publisher recognizes that the U S Government retains a nonexclusive, royalty-free license to publish or reproduce the published form of this contribution or to allow others to do so, for U S Government purposes

The Los Alamos National Laboratory requests that the publisher identify this article as work performed under the auspices of the U S Department of Energy

Los Alamos

Los Alamos National Laboratory
Los Alamos, New Mexico 87545

DISTRIBUTION OF THIS DOCUMENT IS UNLIMITED

FORM NO 836 R4
ST NO 2629 5/81

795 21

Photoconductor Pulse Generators and Sampling Gates for Characterization of High-Speed Devices and Transmission Lines

Nicholas G. Paulter and Robert B. Hammond

Electronics Research Group, Los Alamos National Laboratory
Mail Stop D-429, Los Alamos, New Mexico 87545

Abstract

We describe photoconductive semiconductor devices developed for application in diagnostics of high-speed electronic devices and circuits. Both pulse generation and sampling functions are provided by these ultrafast photoconductors. The photoresponse of different semiconductor materials (GaAs, InP, Si) that have been ion bombarded (Ar, H, He, Ne, O, Si) was investigated and characterized. Response times as short as 1 picosecond have been observed. High frequency propagation characteristics of microstrip and coplanar waveguide transmission lines have been studied and modelled. Application of this measurement technique to the characterization of a microwave GaAs transistor is presented.

Introduction

Photoconductors are enjoying applications as high-speed pulse generators and sampling gates for a variety of diagnostics. Ultrafast photoconductors may be used as fast pulse generators and sampling gates.[1,2] As pulse generators, they may exhibit signal levels in the hundreds of millivolts with pulse widths from one to tens of picoseconds(ps). As fast sampling gates, their sensitivity is decreased by ion beam damage, but the response time is greatly enhanced, providing approximately 1 ps or less[3] temporal windows.

The ultrafast photoconductive device, in conjunction with the correlation measurement scheme, provides electrical measurement systems capable of very high temporal resolution (limited by the FWHM of the sampling device). Also, by use of the CPM laser,[4] there is no jitter between the pulser and sampler laser pulses. Monolithic integration of photoconductive pulsers and samplers in integrated circuits allows one to do on-wafer electrical characterization on any substrate.

The correlation measurement scheme is shown in Fig. 1. The top part of the figure shows a representative structure that we have used in studying pulser and sampler characteristics, transmission line characteristics (both microstrip and coplanar waveguide), and the response of discrete electronic devices. The pulser laser beam is incident on the photoconductor pulser device. The increase in conductivity of this region, due to the incident laser pulse, launches a current pulse onto the transmission line. The other laser beam, the sampler beam, is incident on the sampling device. The increase in conductivity of this region then allows voltage on the transmission line to be sampled on the sampler line. By changing the time of arrival of one optical pulse with respect to the other, we are changing the time of creation of the generated pulse with respect to the sampling time. Varying the delay between the two pulses then allows one to measure a correlation response. The correlation response measured F(τ), is given by the cross-correlation integral of the pulser function, P(t), with the sampler function, S(t). The two plots on Fig. 1 show typical correlations.

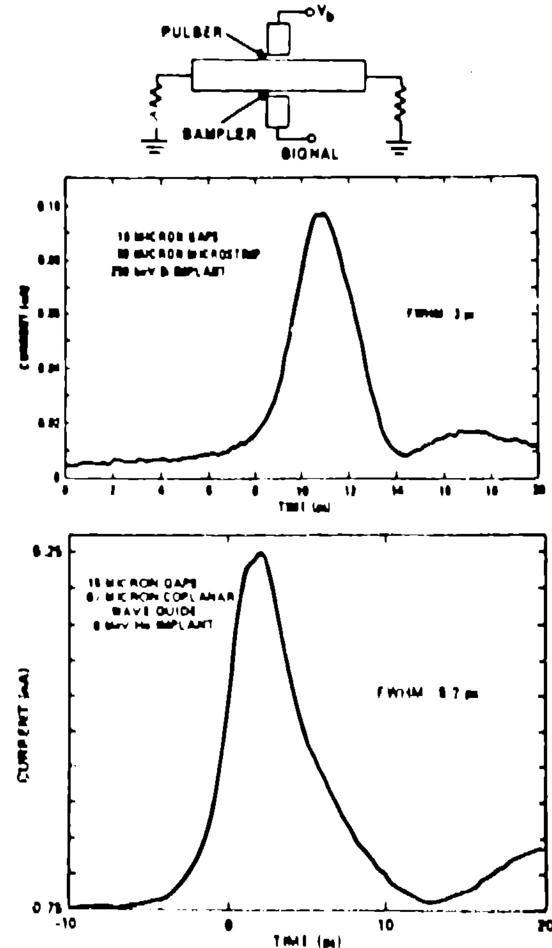

Fig. 1.
Top: Schematic diagram of correlation measurement. Plots show correlations on silicon microstrip and GaAs coplanar waveguide structures.

MASTER

DISTRIBUTION OF THIS DOCUMENT IS UNLIMITED

A principal application for this technique is the characterization of the high speed response of electronic devices,[5] discrete or monolithic. A way to realize this end is shown schematically in Fig. 2. Simply, the electrical pulse generated by the pulser is used to excite the device under test (DUT). The response to this excitation by the DUT, is sampled by the sampling aperture. Varying the delay between pulse generation and sampling provides the correlation measurement. The stimulus to the device and the sampling aperture should both be well characterized in order to accurately determine the device response. A diagram of a photoconductive semiconductor device is shown in Fig. 3.

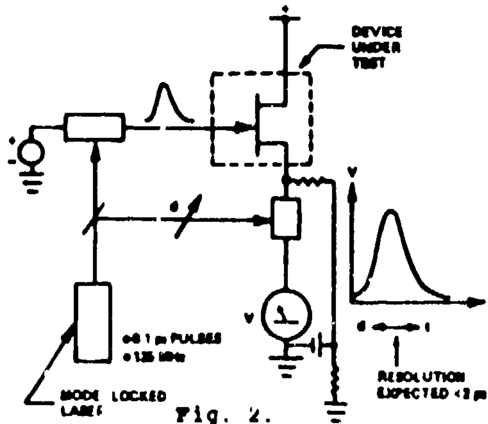

Fig. 2.
Schematic diagram of measurement.

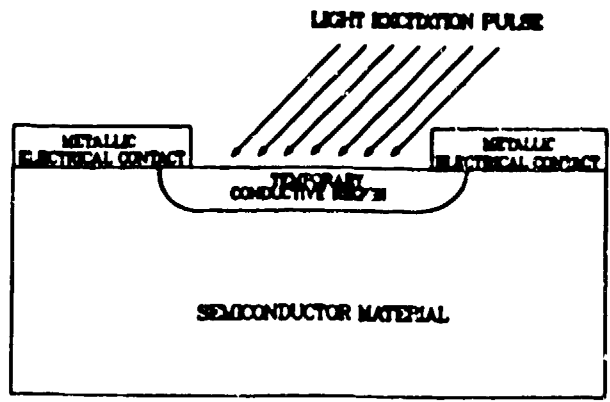

Fig. 3.
Photoconductor schematic diagram.

The substrate may be bulk semiconductor or a semiconductor on insulator. Two metallic electrodes provide the electrical contacts. A light pulse is incident on the semiconductor region between the electrodes. The light pulse increases the conductivity of this region by generating electron-hole pairs. In these experiments, we use a short optical pulse, one that is much shorter than the relaxation time of photogenerated carriers. The duration of the increased photoconductivity is dependent on the carrier relaxation in the excited volume. This volume may be ion-beam damaged to enhance carrier relaxation.[6] The peak current response to short optical pulses is given by:

$$i = (1-r)qv_dE/sW \quad . \qquad (1)$$

where r is the reflectivity of the semiconductor surface, q is the electronic charge, v_d is the carrier drift velocity, (cm/s) E is the photon energy (J), s is the contact spacing (cm), and W is the energy to create an electron-hole pair (eV). The energy to create an electron-hole pair is E_{gap} for optical excitation and is approximately $3E_{gap}$ for energetic-particle excitation. The temporal response is the characteristic carrier relaxation time and the circuit time constant added in quadrature. The circuit time constant is the product of the characteristic impedance of the transmission line and the capacitance of the gap region.

Photoconductor Characterization

The experimental arrangement for the ultrafast characterization is shown in Fig. 4. A CPM laser is used as the excitation light source. One of the beams passes through a mechanical light chopper and an optical delay. Two lock-in amplifiers are used, both locked to the frequency of the light chopper. The variable optical delay is provided by a stepping motor-driven translation stage controlled by an IBM PC. The pulser line is dc biased. The pulse generated at the pulser gap is launched onto the adjacent transmission line. This pulse may be used to excite a DUT, or it may travel along an uninterrupted transmission line, allowing characterization of the transmission line. The voltage on this line is monitored by a lock-in amplifier, giving information on the alignment accuracy of the pulser beam as the translation stage moves through its course. The other beam of the CPM laser is incident on the sampler gap, allowing a small charge to be sampled.

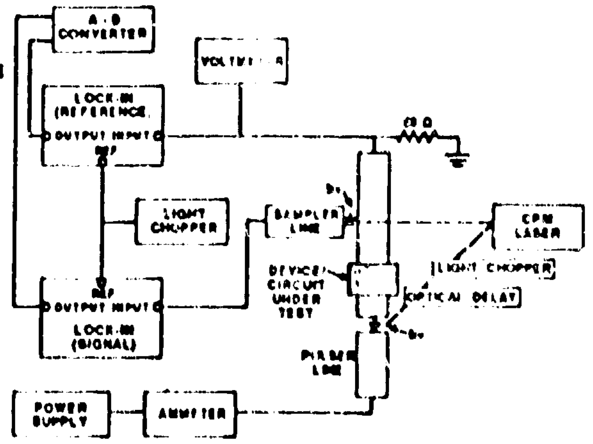

Fig. 4.
Sketch of experimental arrangement.

The output of this line also goes to a lock-in amplifier, this signal yields the correlation response. The output of both lock-in amplifiers goes to an analog-to-digital converter board inside the IBM PC.

The CPM laser operates at a wavelength of 620 nm (corresponding to 0.6 micron absorption length in GaAs, and 2 microns in Si). The repetition rate is 125 MHz. The output of the laser is approximately 80 pJ/pulse with a 200 femtosecond pulsewidth. The sampler sensitivity can be as high as 10 microvolt/hertz$^{1/2}$ for GaAs sampling gates with temporal resolution of 1.3 ps. It is possible to have temporal error due to positioning of the variable delay, but if this occurs, it is only one step (which is 1 micron or 7 fs).

We have studied ultrafast photoconductors fabricated on polycrystalline silicon, Si-on-sapphire (SOS), semi-insulating GaAs (both undoped-LEC and Cr-doped), and semi-insulating InP:Fe wafers. Both microstrip (MS) and coplanar waveguide (CPW) transmission lines were fabricated and tested. The transmission lines were fabricated to have approximately 50 ohm characteristic impedance. The metal contacts were either annealed Al on Si or annealed AuGeNi on GaAs or InP. A mounted Silicon-on-Sapphire (SOS) wafer, with one correlation test structure, ready for testing, is shown in Fig. 5. The photoconductive gap width is 25 microns.

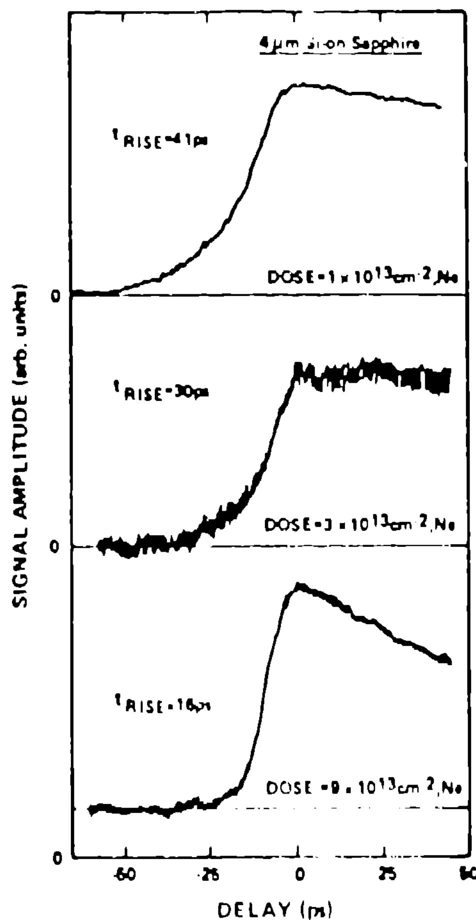

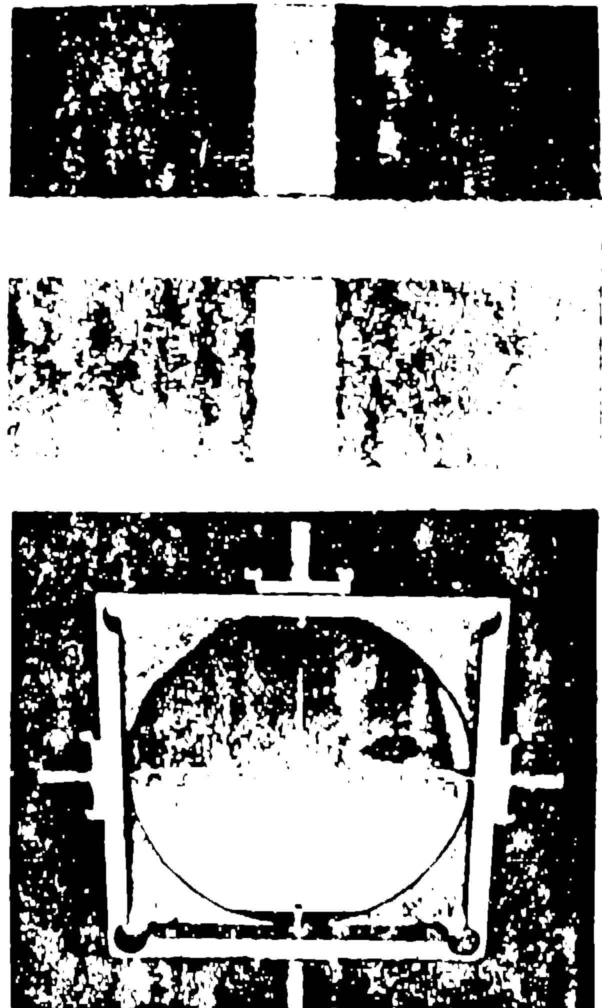

Fig. 5.
Silicon on sapphire correlation structure and data. Left: Correlation data. Top right: Close up of PCEs. Bottom right: Photograph of packaged device.

We performed correlation measurements on this test structure. One of the photoconductive gaps (herein referred to as PCE, Photoconductive Circuit Element) was not damaged in order to provide large step function electrical pulses, the other PCE was ion-beam-damaged with 6 MeV Ne, and functioned as an electronic sampling gate. In all cases, the damage doses were well below the amorphization dose for the material.

Figure 5 shows the cross-correlation results for an SOS (4-micron-thick Si on 325-micron-thick sapphire) microstrip structure where the damage dose has been varied. The rising portion of the correlation measurements show an exponential character and give a measure of the characteristic (e^{-1}) response time in the sampling photoconductor, as indicated in the figure. It is clear that the sampling aperture time decreases with increasing damage dose. The falling portion of the correlations also shows an exponential character and gives a measure of the characteristic response time of the pulsing photoconductor. We can see from this plot that if the response time of the sampling photoconductor were very short, the correlation measurement should give an accurate temporal representation of the electrical pulse produced by the photoconductor pulser.

We performed correlation measurements on our poly-Si, SOS, GaAs, and InP samples with ion beam damage doses varying from 10^{12} to 10^{15} cm^{-2} of various ions.[7,8] The characteristic response times of various semiconductors with damaged sampling photoconductors were determined by the rising edge of the cross-correlations (results are plotted in Fig. 6). For each of the materials studied, the characteristic sampling times decreased with increasing damage dose. This effect is probably due to decreasing carrier lifetimes in the sampling PCEs caused by the increasing densities of recombination centers introduced during ion beam damage. Also, for each of the materials studied, we observed a minimum value for the characteristic sampling time. The limiting values were 5 ps for SOS, 5 ps for GaAs, and 7 ps for InP. The limiting time we observed in these experiments was not due to carrier lifetime in the sampling photoconductors, but rather were due to an intrinsic circuit limit of the structures studied. There are gap capacitances associated with both the pulsing and sampling photoconductors, which in combination with the transmission-line impedance, 50 ohms, introduce Z_0C_{gap} time constants limiting the time response of the circuits studied.[8] We have calculated these Z_0C_{gap} limits for the structures studied: SOS - 4.5 ps, GaAs - 4.8 ps, and InP - 5.3 ps. The calculations are similar to the observed times.

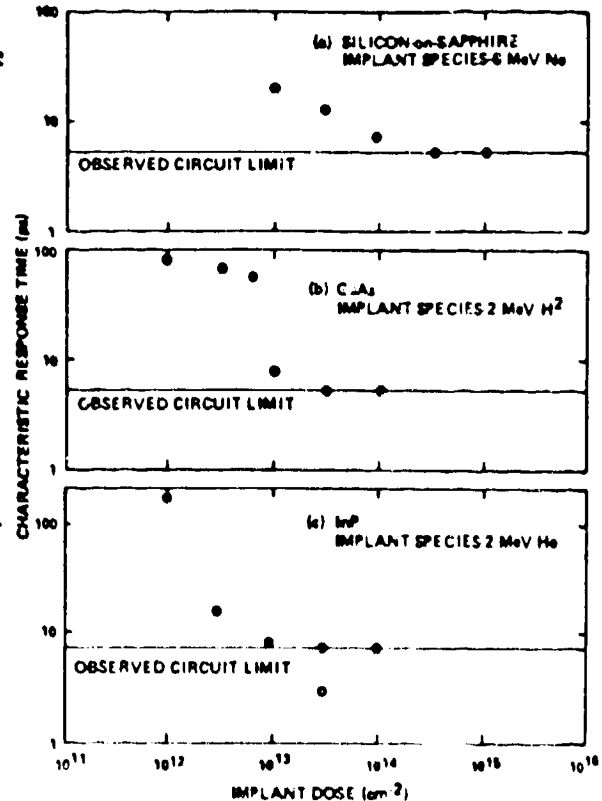

Fig. 6.
Characteristics (e^{-1}) sampling times of radiation-damaged photoconductor sampling gates plotted versus ion beam damage dose. (The hollow data point for InP was taken on a thinned, 175-µm-thick wafer.)

Since Z_0C_{gap} time constants can limit time resolution in correlation measurements on picosecond photoconductors, we considered how these time constants could be reduced. Narrowing the center conductor widths of the microstrip transmission lines will certainly reduce photoconductor gap capacitance, but will also increase transmission line impedance. It thus would have little effect on the Z_0C_{gap} limit of the correlation circuits. However, if the substrate is thinned for a fixed width of center conductor, the impedance will decrease and leave the capacitance unchanged, thereby lowering the Z_0C_{gap} time constant. Thus, a straightforward approach to reducing our observed circuit limits is to thin the substrate wafers. We did this for one measurement on an InP wafer. We thinned it to 175 micron and damaged the sampling photoconductor gap with 2 MeV alpha particles to a fluence of 3×10^{13} cm^{-2}. The result of this measurement, a 3 ps characteristic sampling time, is plotted on the graph in Fig. 7, also circuit-limited correlations for the two thicknesses of InP are shown. The 3 ps sampling time on the thinner wafer is shorter than that on the 400-micron-thick wafers by approximately the same factor as the change in wafer thickness. Further reductions in substrate thickness would allow shorter sampling times.

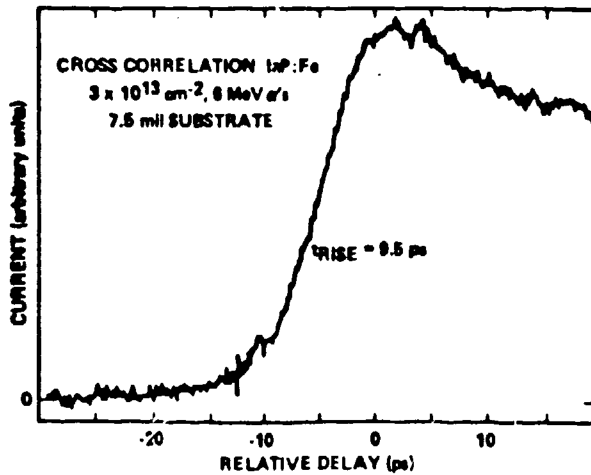

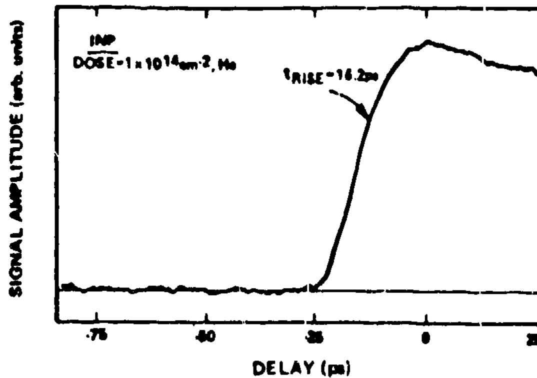

Fig. 7.
Effect of thinning on correlation response of InP:Fe. Top: Without thinning. Bottom: After thinning.

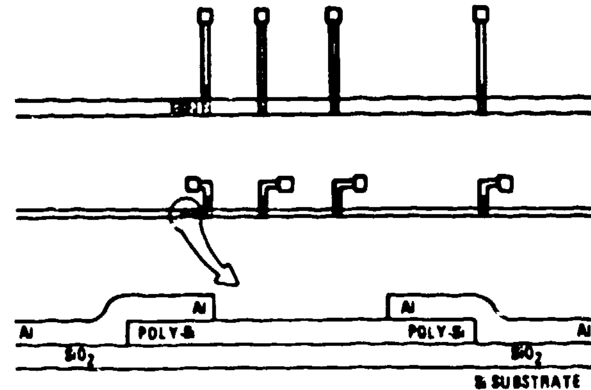

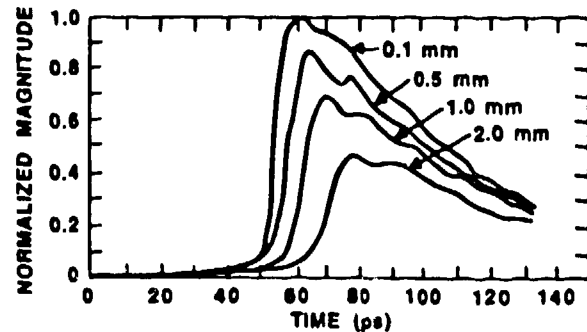

Fig. 8.
Top: Sketch of polysilicon test structure
Botton: Correlation responses taken from each sampler.

Similar measurements done on poly-Si are shown in Fig. 8, along with a diagram of the structure.[9] These wafers had various width transmission lines facilitating measurement of the effect of substrate-to-linewidth ratio on correlation rise time. The samples was damaged with 3×10^{14} cm^{-2} 250 KeV Si. We need not exceed the dose required to realize the circuit limit, since the excess will only degrade our signal levels. Figure 8 shows a correlation of the pulser with various samplers. We can see the degradation of the correlation pulse rise time, indicative of a dispersive line. Also, the waveform magnitude is rapidly decreasing as it propagates down the transmission line. From both the GaAs and poly Si structures in microstrip, we can observe dispersion of the waveform as it propagates down the transmission line. Also, attenuation of the signal is observed, being greater for the lower resistivity Si substrates.

The temporal response of the photoconductor gap is dependent on the PCE material properties, circuit environment, and laser excitation conditions. A first-order model can be derived[9] in terms of the transmission line impedance and gap capacitances and resistance. The time-dependent gap resistance may be obtained by assuming a single exponential describing the carrier relaxation, equal electron and hole capture cross sections, a temporal optical pulse shape ($sech^2$ for CPM laser pulses), and a PCE geometry. This resistance becomes[9]

$$R(t) = x/[q\mu(c+\Delta c(t))AT] \quad , \tag{2}$$

where x is the gap width, c is the carrier concentration, $\Delta c(t)$ is the excess carrier concentration, μ is the average carrier mobility, A is the effective illuminated area, q is the electronic charge, and T is the PCE layer thickness. The PCE response may then

be obtained from R(t), C_{gap}, and transmission line impedance. Fig. 9 is a comparison between the modelled response and measured response of a PCE, which shows that very good agreement exists. At high frequencies our models for impedance and capacitance are not accurate. The higher frequency content manifests itself on the fast rising edge of the correlation signals. We can see from the figure that the model does not describe the performance well in this regime.

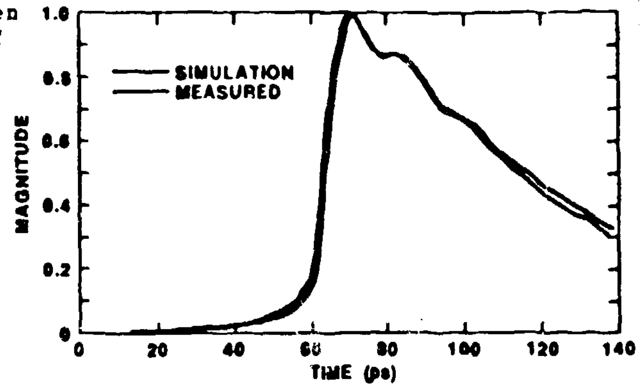

Fig. 9.
Comparison of modelled and measured correlation response.

Transmission Line Characterization

Using the photoconductor pulse generators and sampling gates discussed previously, we were able to experimentally investigate pulse dispersion in various microwave transmission line structures using different material systems. By creating multiple sampling PCEs, both adjacent to, and at various distances from the pulser PCE, we were able to compare pulse rise times after various propagation distances. The results of these measurements on GaAs microstrip lines are shown in Fig. 10. The first pulse, sampled directly across the strip line, shows a rise time of 11.7 ps. After 2.5 mm of propagation, the rise time has degraded to 16 ps, and after 6 mm of propagation, the rise time has degraded to 20 ps. The long "foot" which precedes the second and third pulses is characteristic of geometric dispersion in microstrip transmission lines.

We expect to see significant dispersion of a pulse with 11.7-ps rise time in this microstrip structure because the highest dispersion-free operating frequency of our transmission lines was approximately 13 GHz, while the rising portion of the pulse contained frequencies at least up to our measurement limit of approximately 30 GHz. To obtain dispersion-free pulse propagation at millimeter-wave frequencies requires wafers of 50-micron thickness, increasing greatly the handling problem associated with more fragile semiconductors.

Recent studies of the signal propagation characteristics of microstrip transmission lines allows accurate calculations of the effects of dispersion and loss on pulse propagation. The time response of the transmission line can be shown to be:[10]

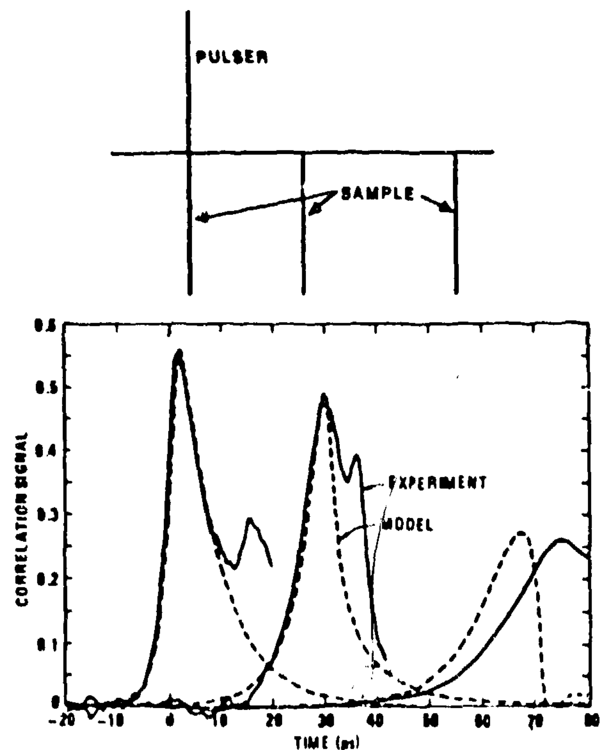

Fig. 10.
Top: Structure used to study dispersion in microstrip. Bottom: Measured and calculated waveforms are plotted.

$$V(z,t) = F^{-1}\{\exp[(\alpha + j\beta)z]*F\{v(0,t)\}\}, \quad (3)$$

where ,

$$\alpha^2 = (-f_1 + \sqrt{f_2})/2 \quad (4)$$

$$\beta^2 = (f_1 + \sqrt{f_2})/2 \quad . \quad (5)$$

where ,

$$f_1 \equiv \beta_0^2 - 4\alpha_c\alpha_d \quad . \quad (6)$$

$$f_2 \equiv (\beta_0^2 + 4\alpha_C^2)*(\beta_0^2 + 4\alpha_d^2) \quad . \quad (7)$$

and α_c and α_d are the conductor and dielectric loss terms under low loss conditions. β is the propogation factor, and V(0,t) is the generated pulse function. F and F^{-1} denote the forward and inverse Fourier transforms. V(z,t) shows frequency dependent effects of loss and dispersion.

Figure 10 shows the correlation between the model for pulse propogation on a microstrip transmission line and the experimentally obtained waveform. Figure 11 shows a calculation of the frequency dependence of the characteristic impedance and of loss of these transmission lines.

In order to address the problems of test structure parasitics and bandwidth limitations, we decided to examine the advantages of coplanar waveguide transmission lines compared to microstrip. A fundamental limitation of microstrip is that the cutoff frequency of the line is determined by the thickness of the semiconductor wafer. It is very difficult to achieve a structure with high cutoff frequency, greater than 100 GHz, because the thin, fragile wafers, are both difficult to fabricate and handle. A way of getting around this is to go to an all-planar transmission line, such as coplanar strips or coplanar waveguide.

Both coplanar strips and coplanar waveguide may be scaled easily to extremely high cutoff frequencies and simultaneously permit photoconductors with very low parasitic capacitances. We chose to study coplanar waveguide[11] rather than coplanar strips because of the very low dispersion we expected from the structure. (Recently low dispersion has shown to also be a property of coplanar strip transmission lines.[3]) In CPW, the ground surrounds the center conductor, making it all-planar and thus lithographically scaleable to small geometries and thus allowing higher cutoff frequencies and lower PCE parasitics. The structure was suggested to us by Dylan Williams of the Department of Electrical Engineering, University of California at Berkeley. Figure 12 is a sketch of the test structure we designed to evaluate coplanar waveguide as a medium for ultra-high-speed measurements on transistors.

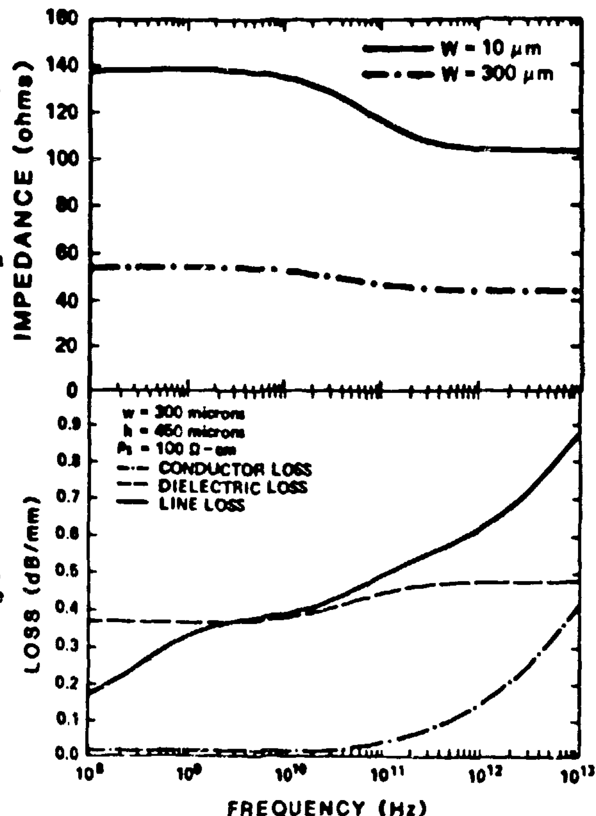

Fig. 11.
Top: Impedance vs frequency plotted for microstrip on Silicon. W is line width, both are for 450 micron substrates. Bottom: Loss is plotted for low resistivity substrates, dielectric loss dominates.

We implemented and studied a coplanar waveguide test structure on GaAs shown in Fig. 12. These test structures had a 50-ohm characteristic impedance and a cutoff frequency of 100 GHz. The test structure contains a photoconductor pulser on the main horizontal transmission line. As in the MS case, multiple sampling PCEs were used to allow the characterization of pulse propagation in the CPW structures.

Figure 12 shows results of pulses measured by all three sampling gates. For these data the photoconductors were damaged with 6-MeV He ions to a dose of 1×10^{15} cm^{-2}. The initial pulse produced has a rise time of 3.3 ps. The most significant result from these data is the fact that the pulse rise time does not degrade as it travels from the pulser 1.2 mm to the third and final photoconductor sampling gate. The rise time remains 3.3 ps. The shape of the pulse changes, however. This is due to the reflection from the wafer backside of a spherical radiated wave produced at the photoconductor pulser. This radiated wave is sampled by the photoconductor samplers along with the wave that is propagated down the transmission line.

These results demonstrate that coplanar waveguide does not suffer from the severe dispersion which one finds in microstrip transmission lines. Figure 13 shows plots of the rise time degradation due to dispersion in microstrip compared to coplanar waveguide. Even for very thin wafers the microstrip shows substantial pulse rise time degradation.

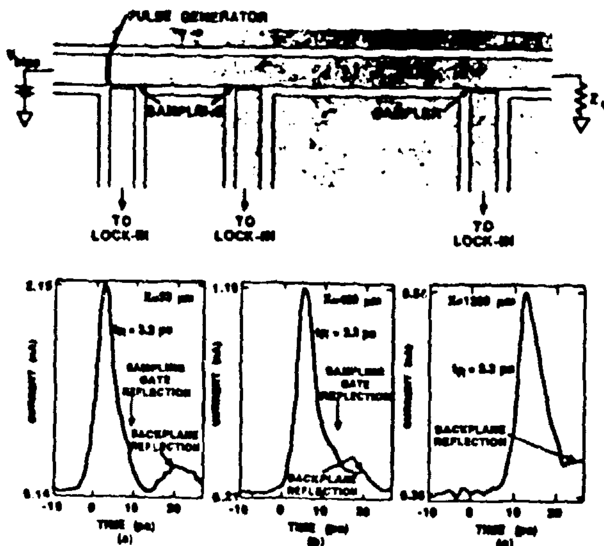

Fig. 12.
Top: Coplanar waveguide test structure.
Bottom: Correlation responses at the 3 samplers.

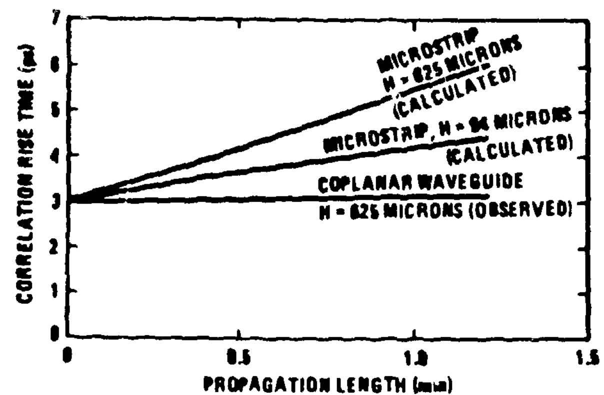

Fig. 13.
Microstrip vs coplanar waveguide correlation risetime dispersion. H is substrate thickness. All systems approximately 50 ohms.

It is also important to note that the backside reflection seen in the data of Figure 12 can certainly interfere with measurements of transistor transient response. However, here coplanar waveguide again has an advantage over microstrip in that the backside reflection can, in principle, be eliminated by removing the metallization and by placing the wafer on a thick substrate of insulating material with similar dielectric constant to GaAs.

It is possible, using a circuit model for photoconductors developed by D. H. Auston,[8] to extract the sampling gate aperture function as well as the actual voltage pulse on the transmission line from the measured correlation data. Figure 14 shows the results of the data deconvolution performed on the correlation shown in Figure 12. We find that the sampling aperture function has a smooth shape and a FWHM of 2.2 ps. We can use the power spectrum of this aperture function to determine the frequency response of the sampling gate. The 3-dB measurement bandwidth is found to be 103 GHz (Fig. 14).[11]

We also find that the actual voltage pulse produced by the photoconductor pulser has a rise time of 2.1 ps and a FWHM of 4.1 ps. The power spectrum of this pulse has a very nice form similar to the power spectrum of the sampling-gate aperture function. That is, its power content is frequency independent below about 53 GHz. Above this frequency it experiences a slow roll-off in power. This pulse, because it is very short and because it has a broad spectral content, is ideal to use to characterize GaAs devices and circuits over a broad frequency range. The short length of the pulse makes it ideal for separating spectral information in the time-domain and thus eliminating effects from unwanted reflections, as is done in conventional time domain reflectometry.

Discrete Device Characterization

Before studying a discrete device, we first characterized the effect of bond wires which we were to use in making electrical connection to the DUT. Here we used 25 micron-diameter Au-wire bonds. Figure 15 compares the pulses propagated along a high-quality microstrip transmission line to pulses that have passed through a short length (1.25 mm) of bond wire. The differences are clearly measurable but not dramatic. They suggest that short bond wire connections might be made successfully to microwave transistors without degrading input and output pulse rise times. However, it is important to note that the transmission line impedance for these data was approximately 80 ohms. If the input impedance of the transistor is substantially lower than 80 ohms, then the rise time degradation experienced by the input pulse will be proportionately larger. This is simply because the limiting time constant due to L/Z_0 will be larger. Very low inductance bond wires are necessary to make contact to millimeter-wave transistors.

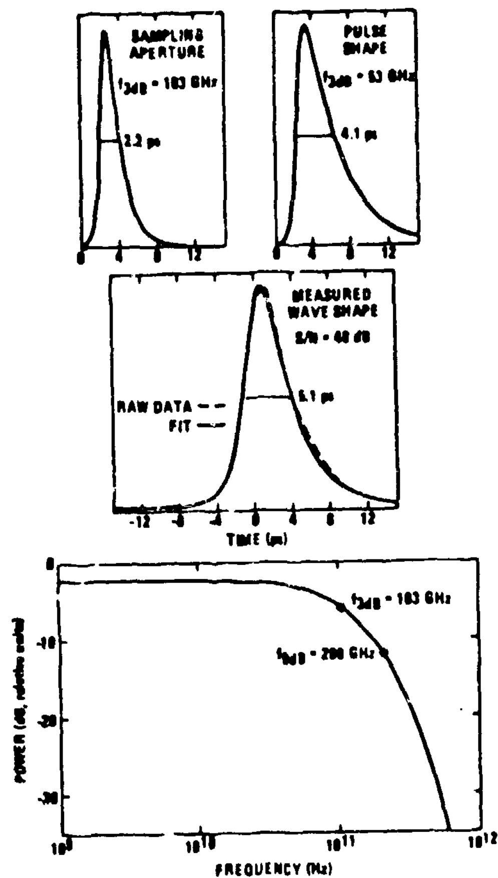

Fig. 14.
Top: Deconvolution of correlation data. Bottom: The power spectrum of the sampling gate aperture function.

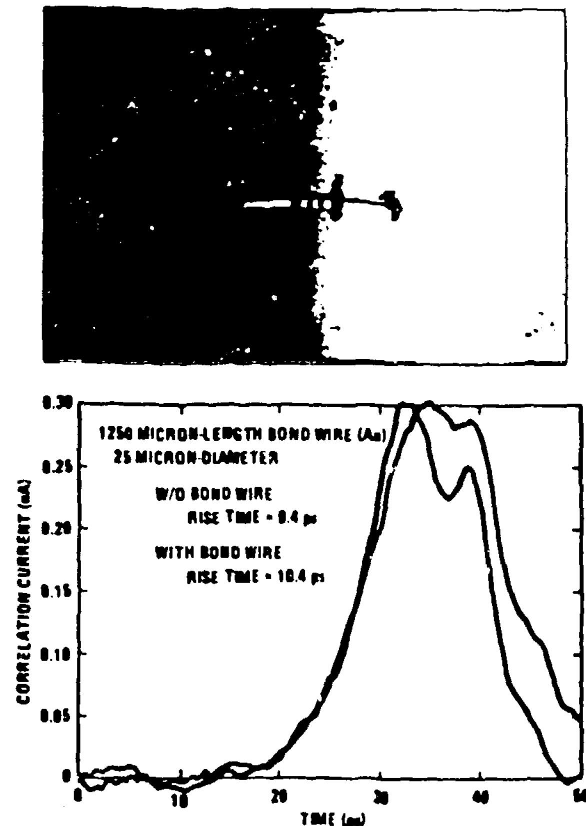

Fig. 15.
Top: Photograph of bond wire. Bottom: Correlation response before insertion of bond wire and after. Transmission line broken before bond wire placement.

Selection of a device for study with ultrafast photoconductors was determined by measurements of the step response with a sampling oscilloscope and gain at 18 GHz with a network analyzer. The Mitsubishi MGF-1403 had the shortest step response and the highest gain at 18 GHz of all the transistors measured. The Mitsubishi MGF-1403 is a 0.3-micron gate-length MESFET with an f_{max} claimed by the manufacturer to be 90 GHz. We measured transconductances of these devices to be between 150 and 200 mS/mm. A mask (Fig. 16) was designed and fabricated for a test structure to perform step response and delay measurements on the FET.

Our optoelectronic test structures were fabricated on 2-in.-diameter, 15-mil-thick, semi-insulating GaAs wafers. Photoconductors were produced as 15-micron gaps between 50-ohm microstrip transmission lines. Sampling photoconductors were damaged with 6-MeV ^{4}He ions to a dose of 10^{15} cm^{-2}. This produced sampling gates with sampling aperture FWHM of approximately 3 ps. GaAs photoconductors on the test structure were not ion-beam damaged and produced pulses with rise times of approximately 7 ps (Fig. 17).

The source electrode of the transistor was connected to ground; the gate voltage was varied between +0.5 to -0.5 V, and the drain voltage between +3.5 to -1.0 V. The test structure permits independent variation of the bias voltages on each of the transistor terminals. Also, the transistor is mounted directly in a high bandwidth, on-wafer, 50-ohm microstrip transmission line. We chose GaAs substrate material for this test structure so that it would be possible to directly implement it in a monolithic structure with any GaAs transistor or circuit.

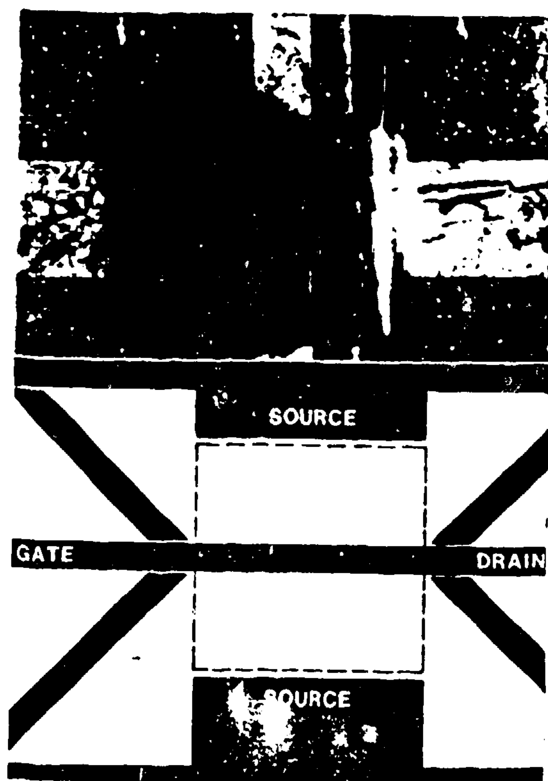

Fig. 16.
Top: Photograph of packaged transistor, Mitsubishi MGF-1403. Bottom: Sketch of test structure used in transistor characterization.

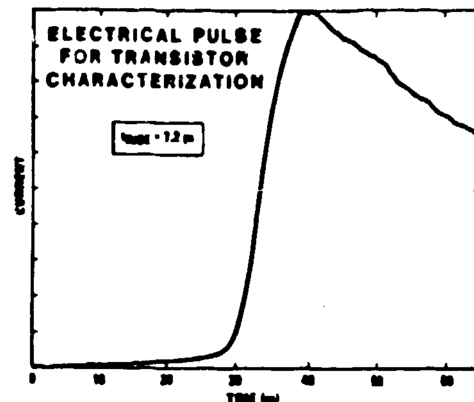

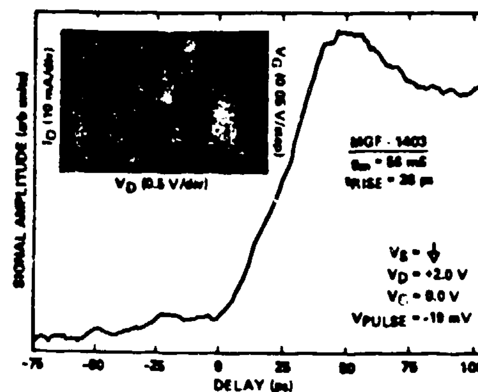

Fig. 17.
Top: Correlation measurement of waveform used to excite FET and sampling aperture. Bottom: Correlation of output at FET drain with sampling aperture.

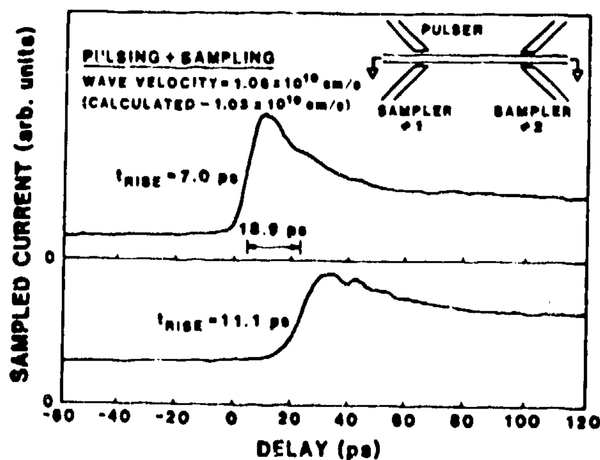

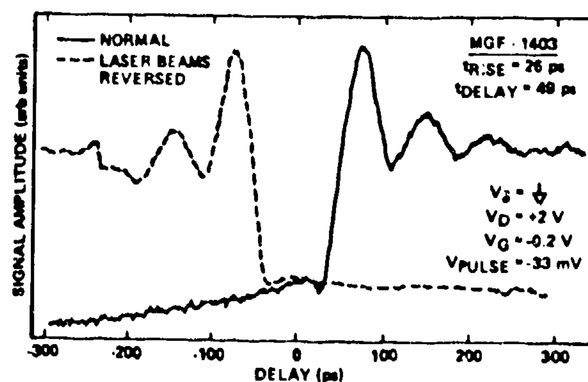

Fig. 18.
Delay measurement. Right: Plot shows delay of waveform before insertion of transistor. Left: Reversal of pulser and sampler beam on Correlation waveform along with normal correlation waveform.

Figure 17 shows a typical step-response measurement on one of the transistors with an inset of the curve-tracer-measured transconductance. The 10% to 90% rise time was 28 ps. The pulse shows some overshoot and ringing that was due to stray inductances at the bonds. The rise time agreed very well with the 31-ps. small-signal rise time predicted from the s-parameter measurements. By reversing the laser beams going to the pulsing and sampling photoconductors, we could accurately measure the signal delay in the transistor plus package. The delay measured for slightly different bias conditions was 49 ps as shown in Fig. 18. It is probable that the 28-ps rise time observed in this transistor is an inherent property of the transistor itself. However, the long delay time, 49 ps, was probably mostly due to delay in the transistor package.

Conclusion

The measurement techniques we have described will aid in the study and development of ultrafast electronic devices and circuits. It will be possible to use our approach to measure device and circuit s-parameters over hundreds of gigahertz in bandwidth in a single measurement, without the complex de-embedding procedures required by network analyzer techniques. Short electrical pulses, a few picoseconds in duration, provide a very broad and flat frequency content for excitation of millimeter-wave devices and circuits. With these pulses it will be possible to measure frequency response simultaneously over hundreds of gigahertz. Also, these short pulses are an ideal way to isolate the reflections from unwanted interconnections by time domain reflectometry.

Our measurements can be implemented directly in a Si or GaAs monolithic circuit. Thus the circuits can be measured directly without mounting and packaging, simplifying testing enormously. We have shown these measurements may be implemented using different microwave transmission lines, and different semiconductor substrate materials. The large signal to noise and high temporal resolution provide extremely high bandwidth measurements.

Acknowledgments

We wish to acknowledge our colleagues that have collaborated in much of the work reported in this paper: Prof. William R. Eisenstadt of the Unversity of Florida, Captain Douglas R. Bowman of the U. S. Military Academy, Prof. Robert W. Dutton of Stanford University, Daniel K. Fitzpatrick of Harris Semiconductor, and Keith R. Goossen of Princeton University. We also acknowledge the financial support of the Department of Energy and the Defense Advanced Research Projects Agency.

References

1. D.H. Auston, A.H. Johnson, P.R. Smith, and J.C. Bean, "Picosecond optoelectronic detection, sampling, and correlation measurements in amorphous semiconductors", Appl. Phys. Lett., 37, 371 (1980).
2. D.H. Auston, "Picosecond optoelectronic switching and gating in silicon", Appl. Phys. Lett., 26, 101 (1975).
3. M.B. Ketchen, D. Grischkowsky, T.C. Chen, C-C. Chi, I.N. Duling,III, N.J. Halas, J-M. Halbout, J.A. Kash, and G.P. Li, "Generation of subpicosecond electrical pulses on coplanar transmission lines", Appl. Phys. Lett., 48, 751 (1986).
4. R.L. Fork, B.I. Greene, and C.V. Shank, "Generation of optical pulses shorter than 0.1 psec by colliding pulse mode locking", Appl. Phys. Lett., 38, 671 (1981).
5. P.R. Smith, D.H. Auston, and W.M. Augustyniak, "Measurement of GaAs field-effect transistor electronic impulse response by picosecond optical electronics", Appl. Phys. Lett., 39, 739 (1981).
6. P.R. Smith, D.H. Auston, A.M. Johnson, and W.M. Augustynaik, "Picosecond photoconductivity in radiation-damaged silicon-on-sapphire films", Appl. Phys. Lett., 38, 47 (1981).
7. R.B. Hammond, N.G. Paulter, and R.S. Wagner, "Observed circuit limits to time resolution in correlation measurements with Si-on-Sapphire, GaAs, and InP picosecond photoconductors", Appl. Phys. Lett., 45, 289 (1984).
8. D.H. Auston, "Impulse response of photoconductors in transmission lines", IEEE Journal of Quantum Electronics, QE-19, 639 (1983).
9. D.R. Bowman, R.B. Hammond, and R.W. Dutton, "New integrated polysilicon photoconductor for ultrafast measurements on silicon", IEEE Proceedings of International Electron Device meeting, Washington, DC 117 (December 1985).
10. K.W. Goossen and R.B. Hammond, "Time domain analysis of picosecond pulse propagation in microstrip interconnections on integrated circuits", submitted to IEEE Transactions on Microwave Theory and Techniques.
11. R.B. Hammond, N.G. Paulter, and A.J. Gibbs, "GaAs photoconductors to characterize picosecond response in GaAs integrated devices and circuits", Proceedings of the International Conference, High Speed Electronics, Stockholm, (Springer-Verlag, New York) 223 (August 1986).